MINISTRY OF EDUCATION AND TRAINING

MINISTRY OF AGRICULTURE AND ENVIRONMENT

VIETNAM ACADEMY FOR WATER RESOURCES

SOUTHERN INSTITUTE OF WATER RESOURCES RESEARCH

LE THANH TRUNG

RESEARCH ON ENHANCING THE BEARING CAPACITY OF BORED PILES BY SHAFT GROUTING

Major: Geotechnical Engineering

Code: 9.58.02.11

DOCTORAL DISSERTATION SUMMARY

Ho Chi Minh City - 2026

The dissertation was completed at:

Southern Institute of Water Resources Research

Scientific supervisors:

1. Dr. Bach Vu Hoang Lan
2. Assoc. Prof. Dr. Nguyen Nghia Hung

Reviewer 1: Assoc. Prof. Dr. Le Ba Vinh

Reviewer 2: Assoc. Prof. Dr. Duong Hong Tham

Reviewer 3: Assoc. Prof. Dr. Truong Quang Thanh

The doctoral dissertation will be defended before the Institute-level Dissertation Evaluation Committee at the Southern Institute of Water Resources Research, 658 Vo Van Kiet Street, Cho Quan Ward, Ho Chi Minh City.

At: ..... hours Date: ...../...../2026

The dissertation is available for reference at:

- National Library of Vietnam
- Library of the Southern Institute of Water Resources Research
- Library of Vietnam Academy for Water Resources

INTRODUCTION

1. Rationale of the Study

Bored-pile grouting technology has been applied in Vietnam for nearly two decades; however, no specific design standards have yet been established. Current calculations rely mainly on empirical equations or foreign references, which are not fully suited to local geological conditions. This study is therefore essential to contribute concrete findings on the effectiveness of shaft grouting for bored piles installed in sandy soils in Ho Chi Minh City, Vietnam.

2. Research Objectives

To investigate the influence of grout injection rate on the increase in the bearing capacity of bored piles installed in sandy ground:

- To evaluate the effect of grout injection rate on pile unit shaft resistance and thereby determine an effective injection rate.
- To propose an equation for predicting the unit shaft resistance of a shaft-grouted bored pile from the corresponding value of an ungrouted pile.
- To propose an approach for simulating the load-settlement (P-S) curve of a shaft-grouted pile in Plaxis using an equivalent diameter (D_{qd}) and a pile-soil interface coefficient (R_{inter}).

3. Research Subject and Scope

- Reinforced concrete bored piles with a diameter of 0.4 m and a length of 3.0 m, installed in loose fine sand in Tan Uyen Ward, Ho Chi Minh City.
- The unit shaft resistance and axial bearing capacity of the piles are investigated under varying grout injection rates; the effects of lateral loading, grouting pressure, and grout mix proportions are not considered.

4. Main Research Content

The research content comprises: (1) a review of studies on enhancing the bearing capacity of bored piles by shaft grouting; (2) the theoretical basis for determining the shaft resistance of shaft-grouted bored piles; (3) the design, construction, testing, and analysis of pile static load tests; (4) the development, calibration, and verification of an equation for predicting unit shaft resistance; and (5) numerical simulation of pile static load tests using PLAXIS 3D and the proposal of a modeling approach for shaft-grouted piles.

5. Research Methods

- Theoretical method: Review, analysis, and synthesis of relevant literature.
- Experimental method: Static pile load testing.
- Data-processing method: Analysis of experimental data.
- Numerical method: Modeling static pile load tests using PLAXIS 3D

6. Novel Contributions of the Dissertation

(1) Quantified the influence of grout injection rate on the unit shaft resistance and ultimate axial bearing capacity of bored piles installed in loose fine sand through instrumented static load tests with strain measurements along the pile shafts.

(2) Proposed an empirical equation for predicting the unit shaft resistance of a shaft-grouted bored pile from the corresponding value of an ungrouted pile, accounting for the effects of grout injection rate and grouting elevation.

(3) Proposed an approach combining an equivalent diameter with the pile–soil interface coefficient to simulate the load–settlement curve of a shaft-grouted bored pile using PLAXIS 3D.

7. Dissertation structure

In addition to the Introduction, Conclusions and Recommendations,

References, and Appendices, the dissertation consists of four main chapters.

CHAPTER 1. LITERATURE REVIEW ON ENHANCING THE BEARING CAPACITY OF BORED PILES BY SHAFT GROUTING

1.1 Overview of Bored Piles

1.2 Overview of Shaft-Grouting Technology

1.3 International Studies on Shaft-Grouted Piles

A synthesis of experimental and finite-element studies worldwide indicates that: (i) grouting markedly increases pile shaft resistance; and (ii) its effectiveness depends on soil type, grouting pressure, and grout injection rate. However, the reported findings remain fragmented.

1.3.1 Field experimental studies

1.3.2 Finite-element modeling studies

1.4 Studies in Vietnam on Shaft-Grouted Piles

Domestic studies are primarily based on: (i) field tests (static pile load tests and O-cell tests); and (ii) finite-element numerical modeling using Plaxis. However, their results are difficult to apply directly to the various soil conditions encountered in Vietnam.

1.5 Mechanisms governing the increase in the shaft resistance of bored piles due to shaft grouting

Three principal mechanisms are involved: (i) an increase in effective normal stress around the pile shaft; (ii) an increase in the pile-soil interface friction coefficient; and (iii) improvement in the mechanical properties of the surrounding soil.

1.6 Chapter 1 remarks

Grouting technology is clearly effective in increasing pile bearing capacity. Nevertheless, a quantitative model suitable for sandy ground in

Vietnam is still lacking. This provides the basis for the research undertaken in this dissertation.

CHAPTER 2. THEORETICAL BASIS FOR DETERMINING THE BEARING CAPACITY AND UNIT SHAFT RESISTANCE OF SHAFT GROUTED BORED PILES

2.1 Theoretical basis for determining the bearing capacity of bored piles under ground conditions in accordance with TCVN 10304:2025

2.1.1 Determination of pile bearing capacity based on ground conditions

The characteristic pile bearing capacity Rk under ground conditions is determined from the unit base resistance qb of the soil beneath the pile tip and the unit shaft resistance fi of each soil layer.

2.1.2 Determination of unit shaft resistance from Physico-Mechanical Properties of Soil

2.1.3 Determination of unit shaft resistance from standard penetration test (SPT) results

2.2 Theoretical Basis for Determining Pile Bearing Capacity by Static Load Testing

2.3 Theoretical Basis for Determining Unit Shaft Resistance from Instrumented Static Load Tests with Pile-Shaft Strain Measurements

An instrumented static load test utilizes strain gauges (SG) installed at various depths along the pile shaft to determine the distribution of axial force during loading. Based on these measurements, the shaft resistance and base resistance components of the test pile can be evaluated. Compared with relying solely on the load–settlement curve to determine

ultimate bearing capacity, strain-instrumented static load testing provides a more accurate assessment of the pile load-transfer mechanism.

2.4 Theoretical Basis for Numerical Modeling of Shaft-Grouted Bored Piles

The finite-element method (FEM) is used to simulate pile static load tests and thereby establish pile load–settlement curves.

2.5 Equations for Determining the Unit Shaft Resistance of Shaft-Grouted Bored Piles

2.6 Chapter 2 remarks

Chapter 2 presents methods for determining the ultimate bearing capacity of piles; equations for calculating the unit shaft resistance of shaft-grouted and ungrouted bored piles; and the mechanisms by which grouting increases shaft resistance. These provide the basis for the field static load tests and numerical analyses of shaft-grouted bored piles conducted in this dissertation.

CHAPTER 3. DEVELOPMENT OF A STATIC LOAD TEST PROGRAM TO ANALYZE THE BEARING-CAPACITY IMPROVEMENT OF SHAFT-GROUTED BORED PILES

3.1 Development of the Experimental Model

3.1.1 Geological Conditions at the Test Site

The experimental program was conducted on a vacant site within the Tan Uyen Training Ground of Engineer Officer School, Tan Uyen Ward, Ho Chi Minh City. The particle-size composition comprised 78.8% sand, 10.9% clay, 9.3% silt, and 0.9% gravel. Standard Penetration Test (SPT) N-values of 2, 4, and 7 were recorded at depths of 0.9, 2.4, and 3.9 m, respectively, with an average value of 4. The site ground consists of loose fine sand. The particle-size distribution curve of the soil at the test site is

shown in Figure 3.2.

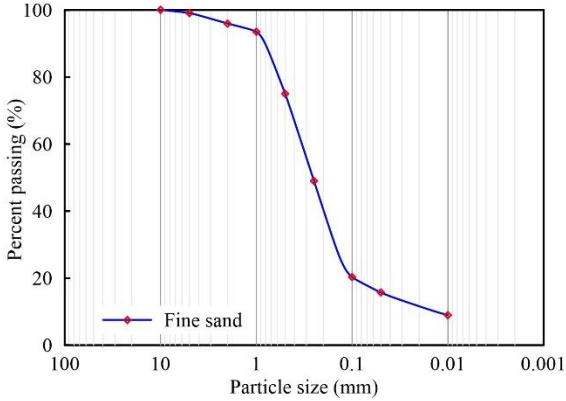
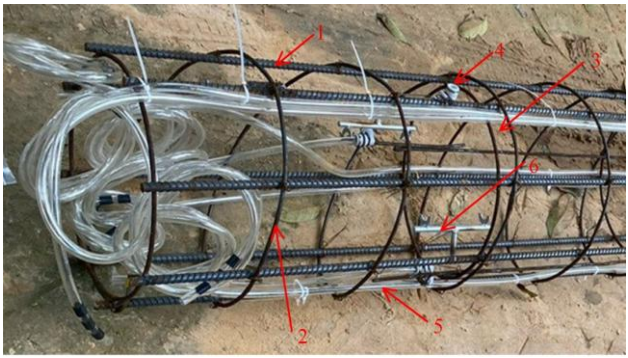


Figure 3.2. Particle-size distribution curve of the soil at the test site

3.1.2 Scale, Configuration, and Construction of the Test Piles

To satisfy measurement-accuracy requirements within the available budget, static load tests were performed on four bored piles (D = 0.4 m; L = 3.0 m), comprising one ungrouted pile and three shaft-grouted piles with grout injection rates IR = 20, 35, and 50 L/m². Each test pile was instrumented with strain gauges (SG) at three different elevations to measure axial strain along the pile shaft (Figures 3.4 and 3.5).



1. Main reinforcement
2. Spiral reinforcement
3. Longitudinal reinforcement bar
4. Grout outlet
5. Grout delivery pipe
6. Strain-gauge installation location

Figure 3.4. Bored-pile reinforcement cage fabricated in the workshop

The piles were constructed in accordance with TCVN 9395:2012. Grout pipes were arranged at elevations of -0.5, -1.5, and -2.5 m. The

grout outlets were opened by pressurized water 24 hours after pile concreting, and shaft grouting at different injection rates was carried out 3 days later.

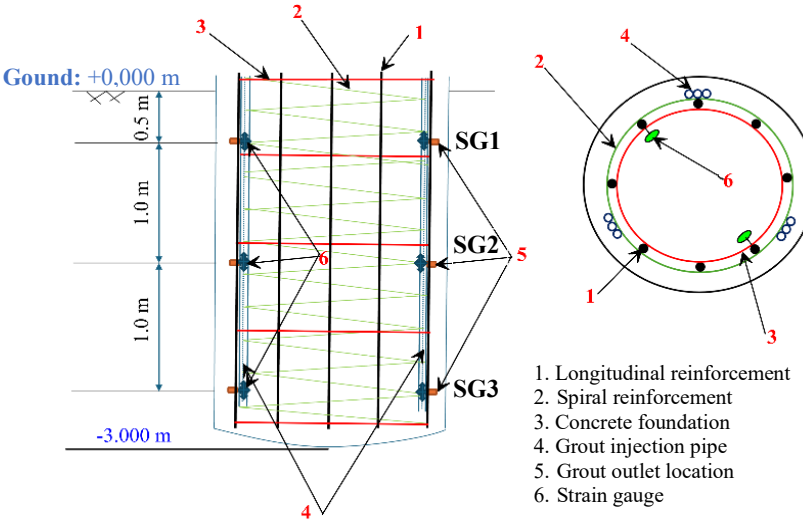


Figure 3.5. Configuration of the test piles

3.2 Pile Static Load Tests Combined with Strain Measurements

3.2.1 Test objectives

3.2.2 Determination of Test Loads

3.2.3 Test Program and Loading Sequence

The pile static load tests followed the rapid load test procedure of ASTM D1143 to minimize stress relaxation effects during strain measurement. The test instrumentation was arranged as shown in Figure 3.9. At each load increment, pile-head displacement, applied load, and strain were recorded to determine the ultimate bearing capacity and unit shaft resistance of each pile segment.



Notation: 1. Longitudinal reinforcement
2. Spiral reinforcement
3. Concrete foundation
4. Grout injection pipe
5. Grout outlet location
6. Strain gauge
7. Reference-beam anchor pile
8. Pile displacement transducer
9. Anchor pile
10. Test pile
11. Steel base plate
12. Stiffened steel support
13. Load cell
14. Spirit level
15. Inclinometer
16. Pile strain-gauge signal cable
17. Load–settlement (P–S) signal cable
18. Sensor support frame

Figure 3.9. Installation of pile static load test equipment

3.2.4 Construction of the Field Static Load Test System

Reaction system: four anchor piles, I400 - I250 reaction beams, and a 40-ton hydraulic jack. Measurement and data-acquisition devices comprised a load cell and displacement gauges, with the test data recorded by a data logger.

3.3 Test Results and Data Analysis of Instrumented Static Pile Load Tests

3.3.1 Pile Static Load Test Results

During loading, all test piles were loaded to a level corresponding to a pile-head settlement greater than 20 mm. None of the four piles exhibited plunging failure, and the loading process was therefore terminated. The load-settlement curves of the four test piles are shown in Figure 3.12.

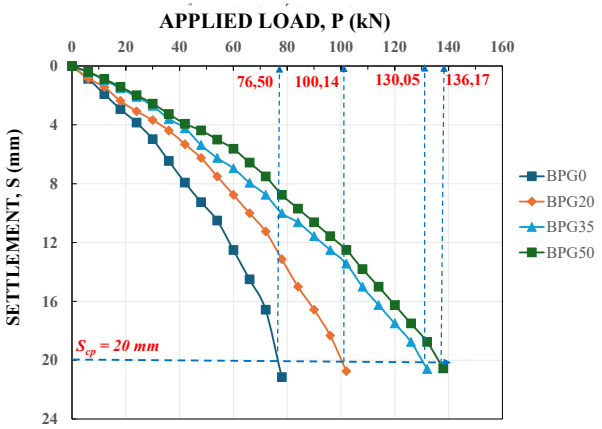


Figure 3.12. P-S curves of the test piles

3.3.2 Analysis of the Effect of Grout Injection Rate on Pile Ultimate Bearing Capacity

According to TCVN 10304:2025, when the P-S curve has no distinct breakpoint, the ultimate bearing capacity (Q_u) is taken as the compressive load (P) corresponding to the allowable settlement (S_{cp}). Q_u increased from 76.50 kN for pile BPG0 to 100.14 kN for BPG20, 130.05 kN for BPG35, and 136.17 kN for BPG50, representing increases by factors of 1.31, 1.70, and 1.78 times, respectively, relative to the ungrouted pile.

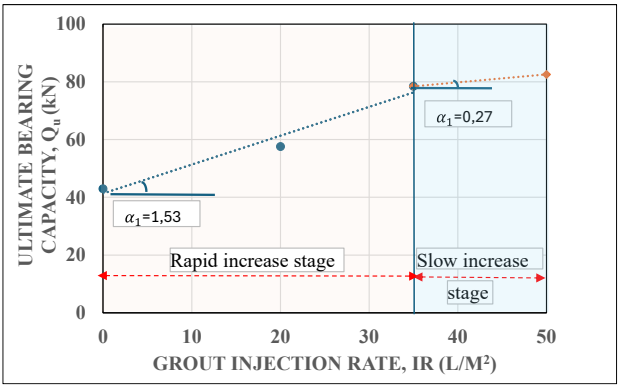


Figure 3.13. Effect of grout injection rate on pile ultimate bearing capacity

The relationship between grout injection rate (*IR*) and ultimate bearing capacity (Q_u), together with the trend line in Figure 3.13, indicates two distinct stages:

(1) For *IR* = 0-35 l/m², the ultimate bearing capacity increases rapidly; with an increase in Q_u of approximately 70% relative to the corresponding value of the ungrouted pile.

(2) For *IR* = 35-50 l/m², Q_u increases slowly, yielding only an additional 8% increase relative to the ungrouted pile. Therefore, *IR* = 35 l/m² can be considered the optimal grout injection rate

3.3.3 Analysis of the Effect of Grout Injection Rate on Pile-Head Displacement

Figure 3.15 shows that the grout injection rate (*IR*) has a pronounced effect on pile-head displacement. At compressive load levels P = 12-36 kN, the differences in pile settlement are not yet distinct. At compressive loads of 48 and 60 kN, the effect of grouting becomes evident: pile BPG0 settles by 9.25 and 12.5 mm, whereas pile BPG50 settles by only 4.38 and 5.63 mm, corresponding to settlement reductions of 53% and 59 %, respectively.

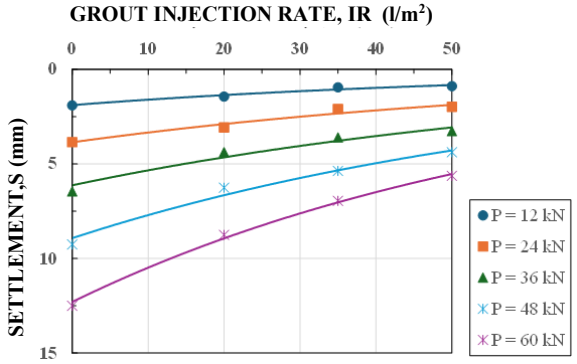


Figure 3.15. Effect of grout injection rate on test-pile settlement at different compressive load levels

3.3.4 Analysis of Axial Strain Measurements

The measured pile strains (Figure 3.16) were relatively small at all load levels, indicating that the pile material remained within the elastic range. The axial stiffness values of test piles BPG0, BPG20, BPG35, and BPG50 were 3.14, 4.58, 6.47, and 6.81 GN, respectively, as determined from the relationship between load and strain measured at SG1 on each pile. The results demonstrate a clear trend of increasing pile stiffness with increasing IR.

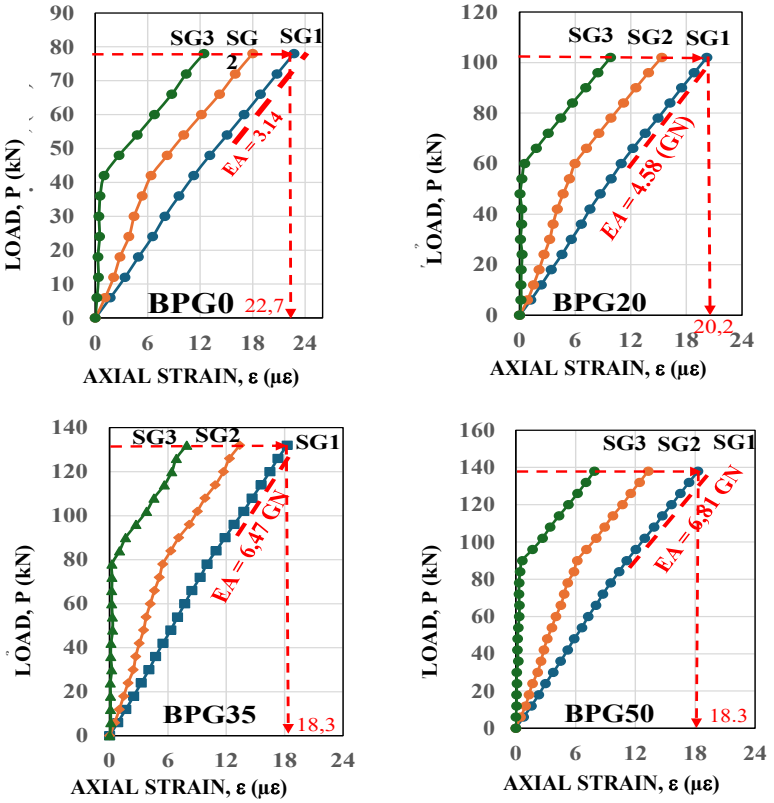


Figure 3.16. Strain data for piles BPG0, BPG20, BPG35, and BPG50

The axial-force distribution diagrams (Figure 3.17), derived from the

measured strains, show that the axial force decreases with depth because of pile–soil shaft friction. At low load levels, the base resistance is almost zero and only shaft resistance is mobilized. As the load increases, the slope of the axial-force-versus-depth curves increases, reflecting greater mobilization of unit shaft resistance. At the final load level, the curves are nearly parallel, indicating that the shaft resistance has been fully mobilized.

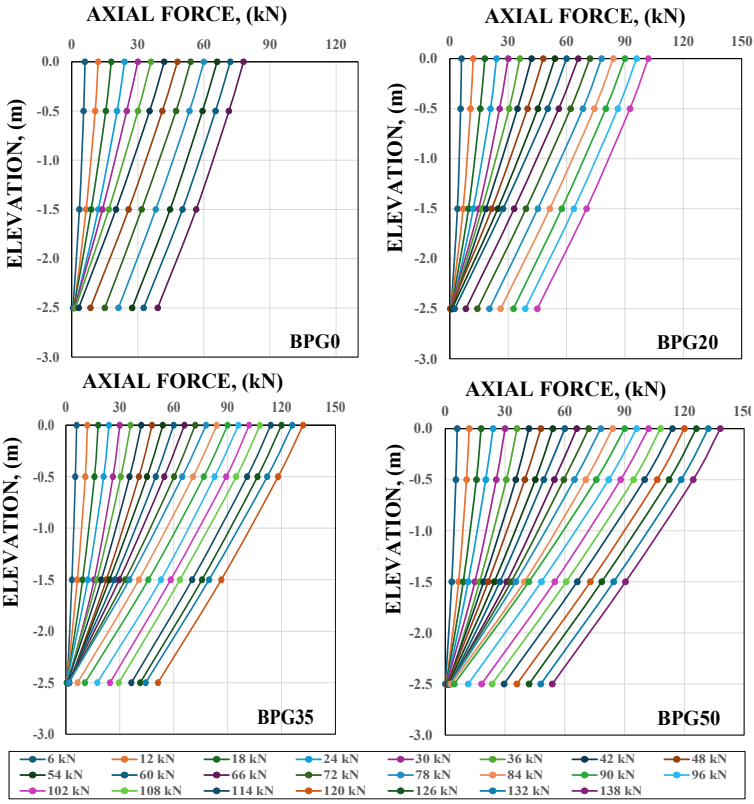


Figure 3.17. Axial-force distribution diagrams for the test piles

As the compressive load drives the pile downward into the soil, the pile-soil friction acts opposite to the direction of movement.

Consequently, the axial force in the pile decreases with depth, from which the unit shaft resistance of each pile segment can be determined (Figure 3.18).

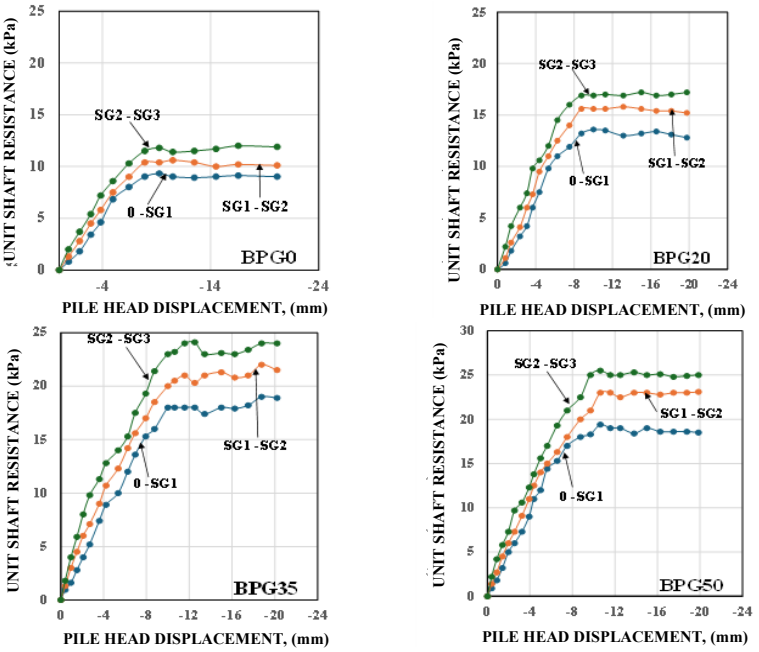


Figure 3.18. Relationship between unit shaft resistance and pile-head displacement

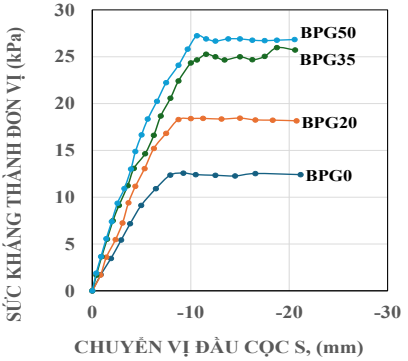


Figure 3.19. Average unit shaft resistance of the piles

The average unit shaft resistance of the ungrouted pile BPG0 was 11.88 kPa, differing by approximately 5% from the value calculated using an SPT-based unit-resistance equation (N_{SPT}). The average unit shaft resistances of the grouted piles BPG20, BPG35, and BPG50 were 18.32, 25.30, and 26.51 kPa, respectively, corresponding to improvement factors of 1.48, 2.04, and 2.14 relative to the ungrouted pile (Figure 3.19).

3.4 Development, Calibration, and Verification of an Equation for Determining Unit Shaft Resistance in Grouted Pile Segments

3.4.1 Development of an equation for determining the unit shaft resistance of grouted pile segments

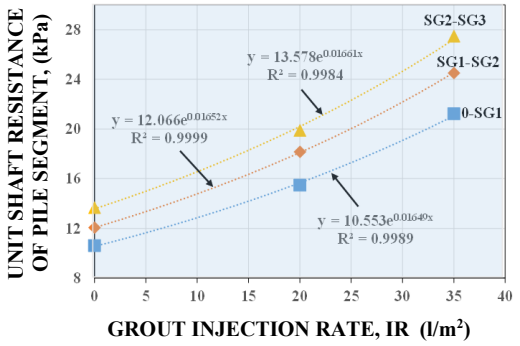


Figure 3.20. Relationship between unit shaft resistance and grout injection rate

From the relationship between unit shaft resistance, grout injection rate (IR = 0-50 L/m²), and grouting depth shown in Figure 3.20, an exponential approximation was adopted to determine the unit shaft resistance fIR of a grouted pile from the corresponding value f_0 of an ungrouted pile:

$$f_{IR} = f_0 . e^{b.IR} \quad (3.2)$$

where: $b = -7.10^{-5}Z + 0.0165$ (3.3)

where f_{IR} and f_0 are the unit shaft resistances corresponding to grout injection rate IR and to the ungrouted pile (IR = 0), respectively; b is a

parameter dependent on grouting elevation; and *IR* (l/m²) is the grout injection rate.

3.4.2 Calibration and Verification of the Proposed Equation for Determining Unit Shaft Resistance in Grouted Pile Segments

To evaluate the proposed equation, static load test data from eight actual projects were used to determine the unit shaft resistance of individual grouted pile segments and the corresponding values for ungrouted pile segments. These data were compared with the values calculated using the proposed Equations (3.2) and (3.3), resulting in an error of approximately 18.7 % (Figure 3.24).

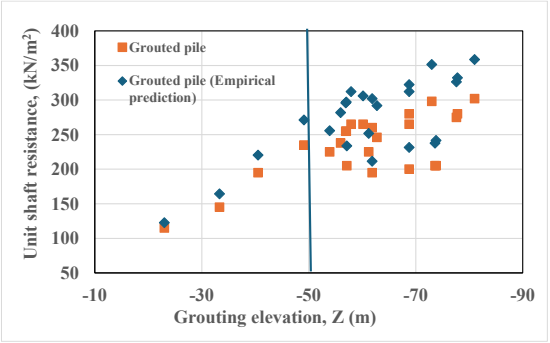


Figure 3.24. Relationship between unit shaft resistance calculated using Equation (3.2) and the corresponding values obtained from static load tests at eight projects

The relatively large discrepancy between the values calculated using Equation (3.2) and the field test results may be attributable to the relatively short length of the piles used in the experimental model. Parameter b was therefore calibrated by comparing the unit shaft resistance of corresponding ungrouted and grouted pile segments obtained from the static load tests at the eight calibration projects:

$$b = -4.10^{-5}Z + 0.0135 \qquad (3.5)$$

where Z is the mean elevation of the grouted pile segment (expressed in metres as a negative value). For elevations deeper than -50 m, Z is taken

as -50 m.

Equation (3.2), with parameter b calculated using Equation (3.5), was then independently verified against test results from two other projects, Song Da Riverside and Song Viet. The difference between the predicted and measured values was 4.83 % (Figure 3.26), demonstrating the high accuracy and applicability of the calibrated equation.

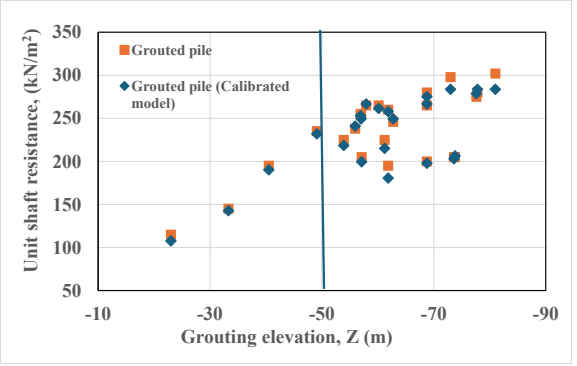


Figure 3.26. Relationship between unit shaft resistance determined using the calibrated equation and the values obtained from data analyses for the Song Da Riverside and Song Viet projects

3.5 Conclusions of Chapter 3

The following conclusions are drawn from the integrated analysis of the field-test results:

- As the grout injection rate increased, the average unit shaft resistance f_{IR} increased by factors of 1.48, 2.04, and 2.14, while the ultimate bearing capacities increased by factors of 1.31, 1.70, and 1.78, respectively, relative to the corresponding values of the ungrouted pile.
- The results show that the shaft resistance of a grouted pile does not increase linearly with grout injection rate. An injection rate IR = 35 l/m² is considered effective for piles installed in the ground conditions at the test site.

- Equations (3.2) and (3.5), which predict the unit shaft resistance (f_s) of a grouted pile from the corresponding value of an ungrouted pile while accounting for grout injection rate and grouting elevation, were calibrated and verified, demonstrating the validity and applicability of the proposed formulation.

CHAPTER 4. SIMULATION OF PILE STATIC LOAD TESTS AND PROPOSED EQUIVALENT-DIAMETER APPROACH FOR SHAFT-GROUTED BORED PILES

4.1 Objectives and Scope of the Numerical Simulation

4.2 Finite-Element Simulation of the Static Pile Load Tests

4.2.1 Development of The Pile-Ground Model

The ground was represented by the Mohr-Coulomb model, which is suitable for establishing the pile load-settlement (P-S) curve. The pile was modeled as a linear-elastic material, consistent with the observed response of the pile material during testing.

4.2.2 Determination of Input Parameters for the Ground and Piles

The input parameters for the ground and piles were determined from laboratory and field tests on soil and pile-concrete specimens.

4.2.3 Boundary Conditions, Finite-Element Mesh, and Calculation Phases

The ground model measured 20 m × 20 m × 10 m, sufficiently large to avoid boundary effects. The mesh was graded from medium at the model boundaries to fine in the soil surrounding the pile. The calculation phases corresponded to the successive load increments applied during the pile static load test.

4.2.4 Goodness-Of-Fit Criterion for Simulation and Test Results

4.3 Simulation of Ungrouted Pile Static Load Test and Calibration of the Interface Coefficient (BPG0)

The static load test of pile BPG0 was simulated first to determine

Rinter such that the simulated load-settlement (P-S) curve approached the measured curve. The trial analyses indicated that R_{inter} = 0.80 was appropriate for the ungrouted pile (Figure 4.2).

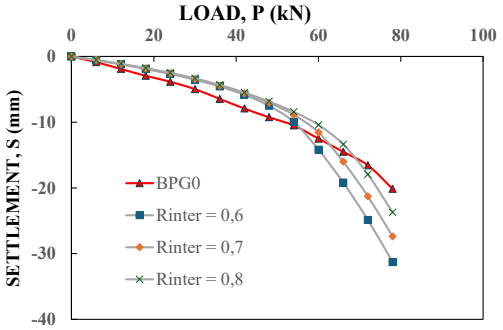


Figure 4.2. Comparison of simulated and measured responses of pile BPG0 for R_{inter} = 0.6-0.8

4.4 Simulation of Shaft Grouted Piles BPG20, BPG35, and BPG50

Grouting increases pile shaft resistance. To simulate this effect efficiently, both the pile-soil contact area and the interface coefficient R_{inter} were increased. The increase in pile-soil contact area along the grouted segments was represented by the equivalent diameter D_{eq}.

4.4.1 Basis and Principles of Equivalent Modeling for Shaft-Grouted Piles

4.4.2 Determination of the Equivalent Diameter Deq of the Grouted Piles

Initially, the ground parameters and R_{inter} = 0.80 were held constant. The diameter of each grouted pile segment was then gradually increased from the original diameter D_0 until the simulated P-S curve matched the corresponding field-test curve. Agreement was assessed using the coefficient of determination ($R^2 \geq 0.95$), from which D_{eq} was determined for each grout injection rate *IR*.

Figures 4.3-4.5 show that the best-fit D_{eq} values for piles BPG20, BPG35, and BPG50 are 0.52, 0.64, and 0.67 m, respectively.

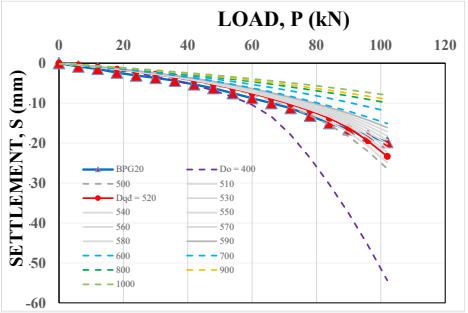


Figure 4.3. P-S curve of grouted pile BPG20 for trial equivalent diameters, R_{inter} = 0.80

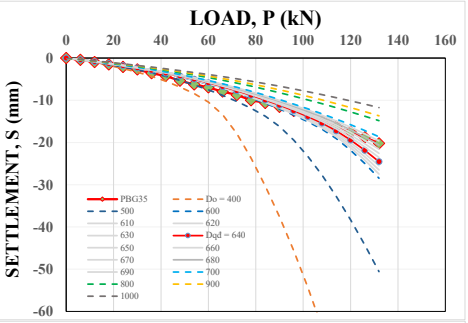


Figure 4.4. P-S curve of grouted pile BPG35 for trial equivalent diameters, R_{inter} = 0.80

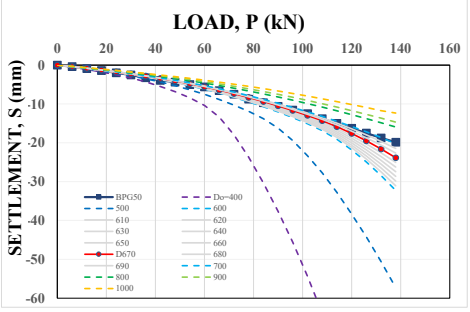


Figure 4.5. P-S curve of grouted pile BPG50 for trial equivalent diameters, R_{inter} = 0.80

4.4.3 Interface Coefficient (Rinter) for the Grouted Piles

To improve simulation accuracy, Rinter was subsequently varied from 0.80 to 1.00 to identify the value appropriate for the grouted pile segments. The appropriate interface coefficient for the grouted pile segments was R_{inter} = 1.00, while ensuring a coefficient of determination $R^2 \geq 0.96$ between the simulated and measured P-S curves (Figures 4.6 and 4.7).

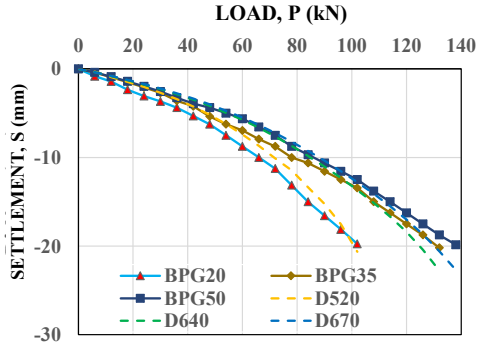


Figure 4.6. P-S curves of the grouted piles using the determined equivalent diameters, R_{inter} = 0.90

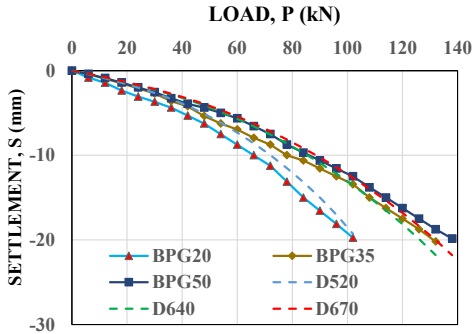


Figure 4.7. P-S curves of the grouted piles using the determined equivalent diameters, R_{inter} = 1.00

4.5 Development of an Equation for Determining the Equivalent Diameter of Grouted Pile Segments in Numerical Simulations

The relationship between D_{eq} and IR was approximated by a quadratic function, as shown in Figure 4.8, with a coefficient of determination R^2 = 0.97.

Accordingly, Equation (4.6) was proposed to calculate the equivalent diameter D_{eq} from the original diameter D_0 of the corresponding ungrouted pile and the grout injection rate IR:

$$D_{eq} = -3.10^{-5}.(IR)^2 + 7.2.10^{-3}.(IR) + D_0 \ \text{(m)} \qquad (4.6)$$

where D_{eq} (m) is the equivalent diameter of a grouted pile at the specified grout injection rate, D_0 (m) is the diameter of the corresponding ungrouted bored pile, and IR is the grout injection rate (l/m²).

Limitations: $IR \leq 50$ l/m²; the grouted pile segment is located in loose fine sand; and the grout has a water-to-cement ratio of 0.66:1.00.

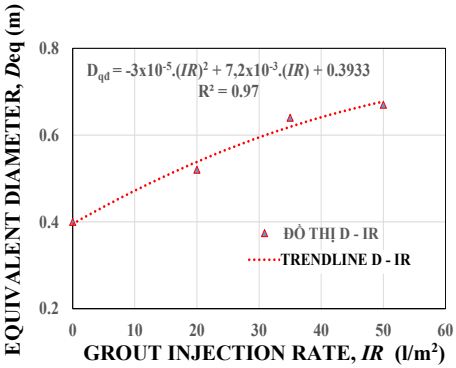


Figure 4.8. Numerically determined relationship between D_{eq} and IR for grouted piles

4.6 Verification of Proposed Equivalent Diameter Equation for Shaft Grouted Pile Segments in Static Load Test Simulation

4.6.1 Verification Principles

4.6.2 Projects Information for Verification

The Friendship Tower project features an ungrouted pile TP1 (D = 1500 mm; L = 80 m) and a grouted pile TP2 (D = 1200 mm; L = 65 m), which was grouted from elevations of -42.20 m to -64.20 m (within a sand layer). The Song Da Riverside project includes an ungrouted pile TP5 (D = 1000 mm; L = 65 m) and a grouted pile TP1 (D = 1200 mm; L = 68 m), grouted from elevations of -45.00 m to -68.00 m (within a sand layer). Static load tests were performed on all piles.

4.6.3 Simulation of Ungrouted Piles for Model Calibration

Plaxis 3D was used to simulate the static load tests of ungrouted piles TP1 (Friendship Tower) and TP5 (Song Da Riverside) to calibrate the ground parameters and R_{inter}.

4.6.4 Application of Equivalent Diameter to Grouted Pile Segments

When setting up the static load test simulations for grouted piles TP2 (Friendship Tower) and TP1 (Song Da Riverside) in PLAXIS 3D, the ground parameters were kept identical to those used for the corresponding ungrouted piles. Meanwhile, the pile diameter along the grouted segment was determined using Equation (4.6), with an interface coefficient R_{inter} =

1.00.

The load–settlement (P–S) curves obtained from field load tests and numerical simulations for grouted piles TP2 (Friendship Tower) and TP1 (Song Da Riverside) are shown in Figures 4.16 and 4.17. The results demonstrate high agreement between measured and simulated curves, with coefficients of determination $R^2 \geq 0.94$.

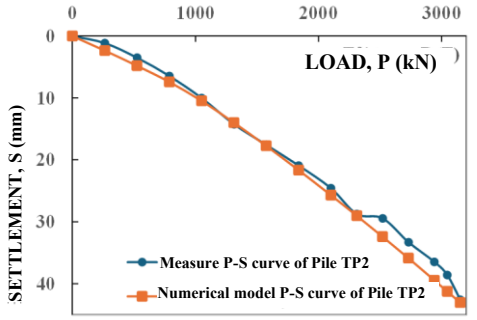


Figure 4.16. Comparison of simulated and measured P-S curves for grouted pile TP2 at Friendship Tower

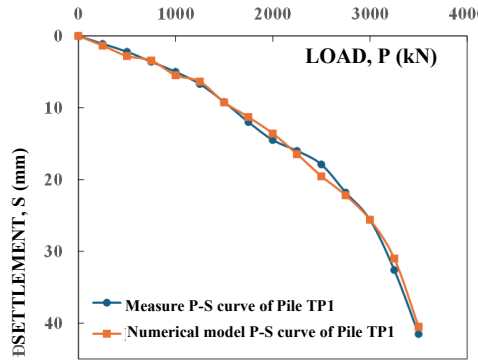


Figure 4.17. Comparison of simulated and measured P-S curves for grouted pile TP1 at Song Da Riverside

4.7 Conclusions of Chapter 4

The implementation of an equivalent diameter D_{eq} and $R_{inter} = 1.00$ for grouted pile segments in Plaxis 3D simulations of pile static load tests produced load-settlement (P-S) curves that agreed closely with the corresponding field-test results.

Equation (4.6) was proposed to determine the equivalent diameter D_{eq}

of pile segments grouted in sandy ground from the original pile diameter D_0 and the grout injection rate, for $IR \leq 50$ l/m².

CONCLUSIONS AND RECOMMENDATIONS

I. CONCLUSIONS

Based on the experimental and numerical results, the main conclusions of the dissertation are as follows:

1. The ultimate bearing capacity (Q_u) of a shaft-grouted pile does not increase linearly with grout injection rate (IR). An injection rate IR = 35 l/m², with a grout water-to-cement ratio of 0.66:1.00, is considered effective for bored piles installed in fine sand ranging from loose to medium-dense conditions (similar to the ground at the test site).
2. The relationship between the unit shaft resistance f_{IR} of a grouted pile segment and the corresponding value f_0 of an ungrouted pile is expressed as:

   $$f_{IR} = f_0 . e^{b \times IR} \text{ where } b = -4.10^{-5} Z + 0.0135$$

   Note: for grouting elevations deeper than -50 m, Z is taken as -50 m.
   Limitations: IR ≤ 35 l/m²; the grouted pile segment is located in loose fine sand; and the grout has a water-to-cement ratio of 0.66:1.00.
3. The implementation of R_{inter} = 1.00 and an equivalent diameter (D_{eq}) for grouted pile segments in Plaxis 3D simulations produces load–settlement (P–S) curves that agree closely with field-test results. The equivalent diameter (D_{eq}) is determined using:

   $$D_{eq} = -3.10^{-5} . (IR)^2 + 7.2.10^{-3} . (IR) + D_0$$

   Limitation: grout injection rate IR ≤ 50 l/m².

II. RECOMMENDATIONS

Based on the derived conclusions, the following recommendations are proposed to guide practical application and future extensions of this research:

1. The equation for determining the unit shaft resistance of a grouted pile

segment from the corresponding ungrouted pile value may be used to predict the ultimate bearing capacity of shaft-grouted bored piles installed in fine sand.

2. The equivalent-diameter (D_{eq}) approach, combined with R_{inter} = 1.00 for pile segments grouted in sandy ground may be adopted to construct load-settlement (P-S) curves using numerical methods.
3. The proposed equations apply to bored piles installed in ground conditions similar to those at the test site and grouted in accordance with the experimental technical requirements. For other geological conditions, the empirical coefficients should be recalibrated and verified.
4. Further experimental and theoretical studies should be conducted in other soil types to refine ultimate bearing capacity prediction methods for shaft-grouted bored piles.

III. FUTURE RESEARCH DIRECTIONS

To support the development of a comprehensive design standard for shaft-grouted piles, the following topics are recommended for future research:

- Investigation of the effects of grout mix proportions and different construction conditions (e.g., drilling fluid types, timing of pressurized-water flushing for outlet opening) on bearing-capacity improvement.
- Evaluation of shaft-grouting effectiveness for piles installed in other soil types, such as clay, loose sand, or gravelly soils.
- Assessment of bearing-capacity gains achieved by shaft-grouting piles with non-circular or alternative cross-sectional geometries.
- Integration of PLAXIS 3D numerical simulations with an expanded field-test database to establish national standard guidelines for the design of shaft-grouted bored piles.

LIST OF PUBLISHED SCIENTIFIC WORKS

1. Le Thanh Trung and Bach Vu Hoang Lan. Equivalent-diameter method for modeling bored piles with shaft grouting. Construction Journal, Ministry of Construction, ISSN 2734-9888, No. 10/2025, pp. 204-207.

2. Le Thanh Trung and Bach Vu Hoang Lan. Effects of shaft-grouting technology on the bearing capacity of bored piles in silty sand. Construction Journal, Ministry of Construction, ISSN 2734-9888, No. 4/2025, pp. 304-308.

3. Le Thanh Trung, Bach Vu Hoang Lan, Nguyen Nghia Hung, and Tran Huu Bang. Numerical modeling of static load tests on shaft-grouted bored piles. Construction Journal, Ministry of Construction, ISSN 2734-9888, No. 10/2021, pp. 82-85.

4. Le Thanh Trung. Analysis of bored-pile static load test results under the geological conditions of District 3, Ho Chi Minh City. Proceedings of the ACEAT 2024 National Scientific Conference: Advances in Construction, Architecture, Economics and Industry 2024, Construction Publishing House, ISBN 978-604-82-8109-0, July 6-7, 2024, pp. 207-216.

5. Trung Le Thanh and Lan Bach Vu Hoang. Field Study on the Effects of Shaft Grouting on the Load-Settlement Behavior of Bored Piles. Indian Geotechnical Journal, Springer Nature, ISSN 0971-9555, Vol. 56(2), pp. 1590-1604.
https://doi.org/10.1007/s40098-025-01266-8

6. Trung Le Thanh, Lan Bach Vu Hoang, and Hai Nguyen Minh. Bearing-Capacity Assessment Shaft Grouting of Barrette Pile by Conventionally Static Loading Test. Springer Nature Singapore Pte Ltd, 2024. In: Lecture Notes in Civil Engineering, ISSN 2366-2557, Vol. 395, pp. 291-305 (Proceedings of the 5th International Conference on Geotechnics for Sustainable Infrastructure Development, Hanoi 2023).
https://doi.org/10.1007/978-981-99-9722-0_19

7. Le Thanh Trung and Nguyen Duc Manh. Static loading tests on PHC piles installed in grouted boreholes. Transport and Communication Science Journal, ISSN 1859-2724, Vol. 72, No. 1 (01/2021), pp. 53-64.